THE ANNALS OF "DUNAREA DE JOS" UNIVERSITY OF GALATI
FASCICLE IX. METALLURGY AND MATERIALS SCIENCE
Nº. 1 - 2024, ISSN 2668-4748; e-ISSN 2668-4756
Article DOI: https://doi.org/10.35219/mms.2024.1.04

COMPARISON OF THE DIFFERENCE IN TEMPERATURE DISTRIBUTION ON THE SURFACE OF TWO ALUMINUM ALLOYS WELDED BY FRICTION STIR WELDING IN DIFFERENT REGIONS AT DIFFERENT LINEAR AND ROTATIONAL SPEEDS

Emad Toma KARASH[1], Amenah Faris HAMID[2]
[1]Northern Technical University / Technical Institute Mosul, Iraq
[2]Northern Technical University / Technical College of Engineering - Refrigeration Department, Iraq
e-mail: [1] emadbane2007@ntu.edu.iq, [2] amina.hamed@ntu.edu.iq

ABSTRACT

Friction stir welding is a modern process that is used commercially on a large scale in various industries and in many countries to connect materials together without reaching the melting point of the metal during the welding process, so it is called the solid-state welding process.

In this research, a three-dimensional mathematical model was designed for friction stir welding of aluminium alloys (AA7075-T6 & AA2024-O) with dimensions (100 x 100 x 6 mm), using (ANSYS 15.0) program to compare the results of temperature distribution with distance from the welding centre to the end of the welded piece, as well as the temperature distribution from the beginning of the welding process to its end, using different rotational speeds (900, 1050, 1200 rpm) and different linear speeds (20, 40, 60, 100 mm/min). In the beginning, the rotational speed was fixed and the linear speed was made variable, and then the linear speed was fixed and the rotational speed was changed.

The experimental results showed that the increase in the rotation speed of the welding tool leads to an increase in the temperatures on the surfaces of the models that were welded by the friction stir welding method. Among the other results obtained, it was found that the increase in the traveling speed of the trolley carrying the models when the stir welding process decreases the temperatures on the surface of the models when the welding process is performed. We note the convergence of the theoretical results with the applied results.

KEYWORDS: AA2024-O, travel speed, ANSYS 15.0, rotational speed, friction stir welding, AA7075-T6

1. Introduction

During the friction stir welding process, the heat generated as a result of friction between the welding tool and the pieces to be welded and the plastic deformation in the welding area leads to changes in the metallurgical and mechanical properties in the welding area. These changes are affected by a number of operational and engineering factors, including the rotational velocity of the welding tool, the travel velocity of the welding table, the design and shape of the welding tool, the amount of heat entering the welding area and some other factors.

There is a different of research that has studied the stir welding processes for aluminium alloys [1]. In this study, a different rotational velocity of the welding tool and a different velocity of the travel velocity of the cart carrying the model were used in order to know the relationship between these variables and prayer in aluminium alloy 7050. The required characteristics were obtained in this study [2]. The researcher studied the temperature of the welding tool with the friction stir welding process and modeling the process for 6061-T6 aluminium alloy. The model is developed to investigate the FSW phenomena inside the tool and work piece and the heat transfer coefficient of the aluminium alloy is improved to (h = 2.0 kW/m^2/kW). The results showed that the temperature the probe is in the middle of the upper surface, 440 °C and 400 °C at the bottom of the probe and the measured surface temperature and the temperature inside the instrument are different by

THE ANNALS OF "DUNAREA DE JOS" UNIVERSITY OF GALATI
FASCICLE IX. METALLURGY AND MATERIALS SCIENCE
Nº. 1 - 2024, ISSN 2668-4748; e-ISSN 2668-4756
Article DOI: https://doi.org/10.35219/mms.2024.1.04

about 40 °C to 50 °C [3]. The researcher has developed an analytical model for aluminium alloy AA 6061-T6 friction stir welding to simulate the contact temperature in the welding process. The results showed that the high heating temperature of the welding process not only improves the welding quality, but also reduces the processing time [4]. The researcher provided an overview and compared the methods of measuring temperature The thermocouples included in the instrument were experimentally evaluated in two different location types. The results showed that the thermocouple temperatures inside the probe had higher readings and a faster response from the thermocouple on the shoulder Both have lower response time and lower temperature readings During the diving process compared to TWT [5]. The researcher carried out a study on the FSW welding tool using the fluid dynamic code, FLAFT, to model a knight in a metal AA2017A box. The results showed that the best flow of materials around the welding tool, in addition to the production of a larger amount of heat in this region, and from this it is possible to estimate the temperatures more accurately through the viscosity generated near the solidus softening region [6]. The researcher studied the effect of tool rotation on Temperatures during the stir welding process for copper and aluminium materials, using the CEL finite element model. The numerical model has been validated by thermal imaging and infrared thermometry. The results showed values close to the experimental temperatures that were found by numerical simulation, and the highest temperature was recorded for the joint line at a distance1 [mm] behind the shoulder of the welder and the direction of the welder turn clockwise compared to the turn of the welder counterclockwise [7]. The researcher has developed a numerical model for aluminium alloy AA2024 and AA7075 based on computational fluid dynamics (CFD) to predict temperature and material distribution, flux during welding process FSW via cylindrical rotation tool Stable plastic viscous laminate. The results indicate when increasing Tool rotation speed (TRS) and shoulder diameter (SD), during the welding process the temperature of the welding area increases and the material flow increases and when the welding speed (WS) is increased. The temperature of the welding area decreases the flow of materials in the stirring area decreases during the welding process [8, 9]. The researcher studied the so-called curing window, through which the quality is good Friction stir welding welds can be produced from AA5083 to AA6082. To this end systematically A set of nine welds equipped using rotation speeds of 280, 560, 840 rpm and Traverse speeds of 100, 200 and 300 mm/min with AA5083 in the advanced side and nine more with reversible material, for comparison a series smaller than the AA5083 - AA5083 and AA6082 - AA6082. It was found through the results that the temperature rise under the welding tool depends on the rotational speed compared to the travel speed [10]. The researcher conducted an experimental and numerical analysis of aluminium alloy 2195 to study the heat flux and temperature of the welding tool and work piece during the stir welding process. The results showed that the temperature resulting from the friction between the welding tool and the work piece is 5% of the tool and the rest of the heat flows into the work piece [11]. The researcher studied the material flow for friction stir welding (UFSW) of low carbon steel and how the welding process is carried out under water using a thermo mechanical model to understand the relationship between the phenomenon of thermal friction during the welding process between the welding tool and the work piece and the knowledge of welding properties. The results showed that the generated heat recorded the highest friction stir welding temperature 1228 ºC and the highest friction stir welding temperature is 1008 °C. Simulation results showed the tensile strength of the steel in the stirring zone (SZ) of the FS Wed joint is higher compared to friction stir welding status. The microstructure of SZ for welded parts in the friction stir welding condition is more accurate than the friction stir welding condition because the water-cooling rate is high [12]. The researcher has developed a model in FSW of alloy AA 7068 with high strength in 3D computational fluid dynamics (CFD) to Study the effect of welding tool pin profile on material flow and temperature improvement Simulations were performed using the k-perturbative RNG model. The higher temperature obtained in the experiment is lower than the temperature obtained by simulation. The hardness was checked in different welds about 71% of the hardness of the base metal was obtained [13]. The researcher studied the heat transfer behavior of friction stir welding of aluminium alloy AA5052-AA6061 and their dimensions are 300 mm in length and 150 mm in width by determining the temperature distribution on the welded aluminium alloys and using the program ANSYS Finite Elements. The results indicate that the temperature distribution for each of the aluminium alloys AA5052 and AA6061 due to the similarity of the properties of the alloys and the maximum temperature resulting in the simulation agree with the results experimental [14]. The researcher has developed a finite element model for the friction stir welding process based on the mechanics of solid materials using ABAQUS to study the material flow for the welding process, particle tracking technology. The simulation results showed that the flow pattern the particles follow around the welder moving in a

THE ANNALS OF "DUNAREA DE JOS" UNIVERSITY OF GALATI
FASCICLE IX. METALLURGY AND MATERIALS SCIENCE
Nº. 1 - 2024, ISSN 2668-4748; e-ISSN 2668-4756
Article DOI: https://doi.org/10.35219/mms.2024.1.04

spiral motion to the upper surface and vortex to the lower part. And the velocity of material flow to the surrounding part the welding tool is higher than the lower part of the welding tool [15]. The researcher welded aluminium alloy 2024-T4 With a thickness of 1.9 mm by friction stirs welding; the tool used in the welding process is FWS-C conical probe and FWS-H hexagonal conical probe. The results for the FSW-C sample show temperatures are high at the bottom of the screw end and the temperature results for the FSW−H sample are the highest stretching temperature, from the probe tip to the adjacent area towards the forward side. The use of a hexagonal probe has a good metal effect, which increases the heat input and improves the flow of materials [16]. The researcher made a model of friction stir welding for AA6061 Alloy and AA5086, and a study of the effect of temperature on the welding tool, the displacement of the tool, and the position of the alloys. The results showed that the temperature increases in the position of the hardest aluminium alloy AA6061 on the advancing side compared to the position of the alloy on the declining side. The displacement of the tool has a significant effect on the temperature [17]. The researcher distributed the temperature on aluminium alloy 6082 during the friction process, welding noise, by placing eight thermocouples, four on the forward side and four on the back side, with different tilt angle and stopping time, the tool rotation speed is constant and travel speed. The results showed a higher temperature in the position of the alloy on the advancing side compared to its position on the retreating side. Many other studies have adopted the study of the effect of rotational speeds, linear speeds, and types of pens on temperature distribution and mechanical properties, and many metals were used, including metals subject to heat treatments, and different and valuable results were drawn for friction welding, especially for aluminium alloys [18-30].

In this study, the results of the effect of these factors on the temperature distribution on the surfaces of the welded models, and the temperature values from the starting of the welding stir friction process to the end of this process, will be presented, as well as a study of the effect of temperature changes on the surfaces of welded models in different places on the hardness resistance of these models.

Experimental work in this model included preparing aluminium sheet models (AA-2024-O & AA-7075-T6) and the models manufactured in the specified places, to know the temperature distribution during welding operation.

2. Experimental work

2.1. Metal Property

In this study, aluminium alloys (AA-2024 – O & AA-7075-T6) heat treated sheets were used as a metal base in this work. – Northern Technical University-Mosul Technical Institute Department of Mechanical Engineering - Mosul. Table 1 shows chemical analysis of alloy component proportions and their comparison with the standard ratios values approved by the European Aluminium Association (EAA). Table (2) shows a comparison of the mechanical properties of the tested alloy (AA 2024–O) with the standard values of the alloy itself according to the American specifications (ASTM E 3-01), Table 3 shown thermal properties of aluminium alloys [30-33].

Table 1. *The chemical composition of aluminium alloys*

Elements / Materials	Zn %	Si %	Fe %	Cu %	Mn %	Mg %	Cr %	Ti %	Al %
Nominal value AA-2024 – T6 [31 - 33]	0.21 - 0.25	0.33 - 0.5	0.41 - 0.5	3.8 - 4.9	0.3 - 0.9	1.2 - 1.8	0.08 - 0.1	0.13 - 0.25	Rem.
Actual value	0.23	0.38	0.47	4.1	0.48	1.62	0.09	0.15	92.48
Nominal value AA-7075 – O [31 - 33]	5.1 - 6.4	0.4 - 1.5	0.15	1.2 - 2	0.3	2.1 - 2.9	0.18 - 0.28	0.2	Rem.
Actual value	5.43	0.32	0.49	1.6	0.28	2.35	0.23	0.18	89.12

Table 2. *Mechanical properties of aluminium alloys*

	Density, Kg/m³	Tensile Yield Strength, MPa	Ultimate Tensile Strength MPa	% EL	Modulus of Elasticity, GPa	Shear modulus, Gpa	Hardness, Vickers	Hardness, Brinell	Passion's ratio, μ
Nominal value, A-2024 [31 - 33]	2780	345	483	10	73.1	28	56	46	0.33
Actual value	2780	95	220	12	73.1	28	57	47	0.33
Nominal value, AA-7075 – T6 [31 - 33]	2810	503	572	5	71.7	26.9	175	150	0.33
Actual value	2840	501	570	5	71.72	26.9	177	153	0.33

Table 3. *Thermal properties of aluminium alloys*

	CTE, Travel 205, c°	Specific heat capacity, $\frac{j}{g.c^{\circ}}$	Thermal conductivity, $\frac{W}{m.c^{\circ}}$	Melting point, c°
Nominal value, AA- 2024 – T6 [31 - 33]	24.7	0.875	121	638
Actual value	24.3	0.873	121	638
Nominal value, AA-7075 – T6 [31 - 33]	52.5	0.96	130	635
Actual value	52.6	0.97	130	635

THE ANNALS OF "DUNAREA DE JOS" UNIVERSITY OF GALATI
FASCICLE IX. METALLURGY AND MATERIALS SCIENCE
Nº. 1 - 2024, ISSN 2668-4748; e-ISSN 2668-4756
Article DOI: https://doi.org/10.35219/mms.2024.1.04

2.2. Machines and equipment used

The traditional vertical milling machine was used to carry out all the friction stir welding operations in the mechanical workshop, and we also manufactured a simple carbon steel fixture tool for the pieces to be welded to fix the pieces during the operations. In the current study, two factors were chosen among the factors of frictional mixing processes, namely the travel velocity of the milling machine table and the rotational velocity of the friction tool, where three rotational velocity (1000, 1225, 1525 rpm) and three travel velocity (30, 40, 60 mm/min) were chosen, and the rotation was the tool is clockwise (CW) to perform the entire process of friction stir welding. Figure 1 shows the milling machine used in the friction stir welding.

Fig. 1. *Milling machine used in the friction stir welding*

A tit device was used to measure temperatures on the surfaces of the welded models, during the friction stir welding process, and the device measures temperatures between (-50-550 °C). Figure 2 shows device that measurers the temperature by distance.

Fig. 2. *Shows device those measurers the temperature by distance*

Tapered threaded left-toothed with a diameter of (18 mm) and a pin with a diameter of (18 mm) and a diameter of (5.5 mm) at the base and (4.7 mm) at the end and a height of (2.9 mm), and using the tilt angle of the welding tool (tilt angle) is (2°) from the vertical axis to obtain a high quality of welding, and the tool rotates clockwise (CW). It is worth mentioning here, that the optimum value of the angle of inclination of the welding tool is within (2°-4°), and Figure 3 shows the shape and dimensions of the welding tools, while Table 4 shows the chemical composition and mechanical properties of the welding tools used in the test, and Tables 4 and 5 types of materials used in the manufacture of welding tools.

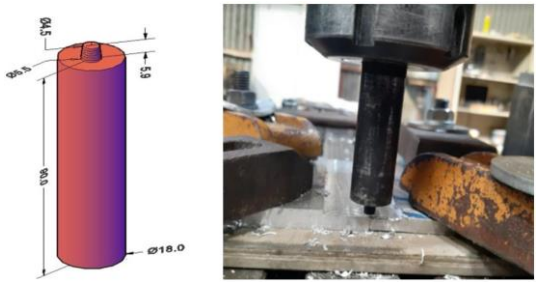

Fig. 3. *shows the shape and dimensions of the welding tool, which are a cylindrical tool with a conical serrated protrusion*

2.3. Materials and working methods

The metal used in this study is two aluminium alloys (AA-2024 - O & AA-7075-T6), which have poor weld ability by fusion welding methods.

The alloy plates with a thickness of (6 mm) were cut into strips and using coolant to avoid affecting their original structure by means of an electric disk saw, and the dimensions were adjusted using a milling machine to obtain the required dimensions (100 * 100 * 6 mm) and prior to the welding stir process. Friction The oxide layer is removed from the surface of the parts to be welded, especially in the joint area, using grinding paper and cleaned with acetone solution to remove dirt and contaminants. (Rolling direction) as shown in Figure 4.

The models prepared by the friction stir welding method were welded at different rotational velocity of the welding tool (1000, 1250, 1525 rpm), as well as the travel velocity of the welding table on which the welded models are fixed (20, 40, 60 mm / min) using a welding tool of length (90 mm).

THE ANNALS OF "DUNAREA DE JOS" UNIVERSITY OF GALATI
FASCICLE IX. METALLURGY AND MATERIALS SCIENCE
Nº. 1 - 2024, ISSN 2668-4748; e-ISSN 2668-4756
Article DOI: https://doi.org/10.35219/mms.2024.1.04

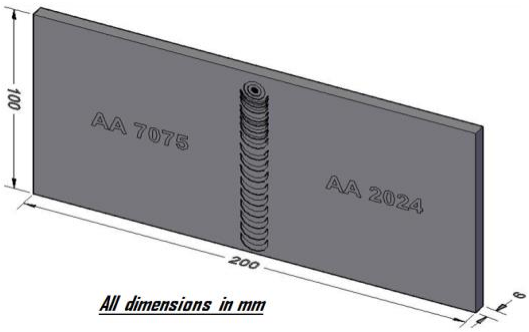

Fig. 4. *Shows the shape and dimensions of the parts to be welded*

2.4. Distributing temperatures when performing friction stir welding

The temperatures were measured on the surfaces of the models when friction mix welding was performed, as in Figure 5, which shows the points where the temperatures were measured for the models that were welded by friction mix welding method. Temperatures were measured using the laser device to measure the temperatures on the surfaces of the models when performing frictional mixing welding operations.

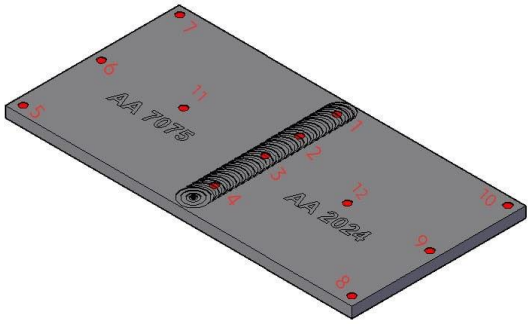

Fig. 5. *Shows the points where the temperatures were measured for the models*

Points on the vertical line were also determined from the starting of the friction stir welding process to the end of the welding process, and the temperatures were measured using a laser device, which are the points (1, 2, 3, 4) in order to study the effect of changing temperatures when changing the travel velocity of the welding cart and the rotational velocity of the tool. Figure 6 shows those points.

The temperatures were taken in five points on one horizontal line, which are the points between (3, 6, 9, 11, and 12) in order to study the distribution of temperatures in the middle of the welded pieces, and the Figure 7, shows those points.

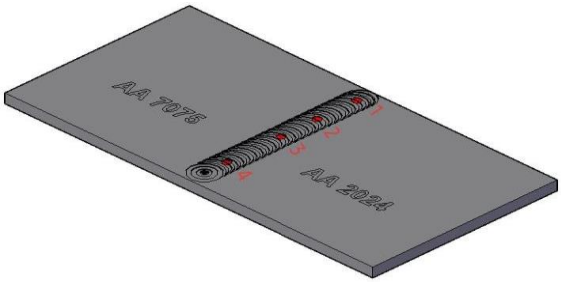

Fig. 6. *shows the vertical points where the temperatures were measured for the models*

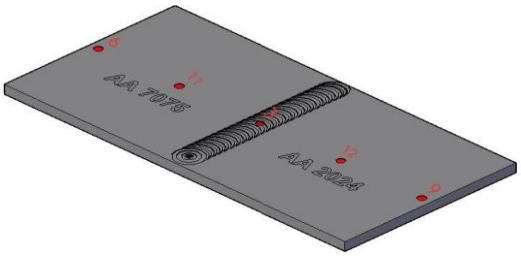

Fig. 7. *shows the horizontal points that have been identified in order to take the temperature values in them*

2.5. Steps to do the friction stir welding process

First, we install the two alloys with each other (1) on the cart of the milling machine, by means of the brackets of the installation tool, and we put under the alloys a sheet of steel to retain heat when performing the friction stir welding process.

Secondly, we tilt the welding tool at an angle of ($\alpha = 2°$) from the vertical axis to obtain a high quality of welding.

Thirdly, we then choose the required travel velocity and rotational velocity, and the chosen travel velocity is (20, 40, 60 mm/min) and rotational velocity (1000, 1225, 1525 rpm) in each process, either the travel velocity or the rotational velocity was changed according to the work platform.

Fourth, we operate the milling machine, and then we carry out the process of lowering the tool weld down until it touches the contact area of the two alloys, and this process continues to go down until the tooth of tool enters the inside of the alloys so that the shoulder of the tool is on the surface of the two alloys by touching them, so that the metal is confined within the concavity on the shoulder of the welding tool, through the rotation of the welding tool, heat is generated and the two alloys are welded together in the contact area between them and the process takes place from starting to end, with the use of a laser device to measure the temperature in the areas identified on the surface of the alloys, and before the

THE ANNALS OF "DUNAREA DE JOS" UNIVERSITY OF GALATI
FASCICLE IX. METALLURGY AND MATERIALS SCIENCE
Nº. 1 - 2024, ISSN 2668-4748; e-ISSN 2668-4756
Article DOI: https://doi.org/10.35219/mms.2024.1.04

welding tool reaches the end of the model by less than two millimetres, the process is stopped, the welding tool is raised and cooled in order to preserve it, Figure 8.

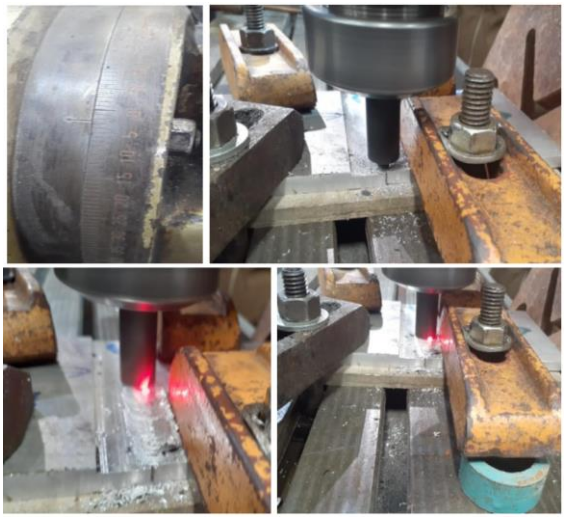

Fig. 8. *It shows the method of fixing the alloys, calibration and the welding process from starting to end*

3. Results and discussion

3.1. Distributing the degree of heat to the surfaces of welded patterns

After preparing the models that were composed of aluminium ingots (AA-2024 - O) and nine other models of aluminium ingots (AA-7075 T6) and after welding these pieces together by friction stir welding, at different rotational and travel velocities, welded models were obtained.

The results of the temperature distribution test on the surfaces of the models when the friction stir welding is performed for the samples appear in the Table 4.

Table 4. *shows the distribution of temperatures during the friction stir welding process on the models*

Model	Rotational velocity (rpm)	travel velocity (mm/min)	T1	T2	T3	T4	T5	T6	T7	T8	T9	T10	T11	T12
1	1000	30	230	290	329	358	50	54	59	50	52	57	158	162
2		40	214	269	307	325	50	53	57	50	51	55	145	155
3		60	189	243	275	297	50	51	55	50	50	53	138	146
4	1225	30	248	324	357	375	50	58	65	50	56	62	188	182
5		40	232	300	334	348	50	56	63	50	54	60	175	175
6		60	214	273	308	326	50	55	60	50	52	58	162	166
7	1525	30	287	347	373	385	50	62	70	50	59	68	198	192
8		40	265	328	353	363	50	60	68	50	57	65	185	185
9		60	232	305	329	340	50	59	65	50	55	62	172	176

3.2. Effect of constant of rotational velocity and change of travel velocity

The results obtained in Figure 6 were analysed in the Excel program to compare these results with the Figures 9 and 10. Figure 9 shows the relationship between the time spent in the friction stir welding process of the two alloys from the starting of the welding process to its end with the temperature distribution on the welded models on the vertical line of the welding process from the starting point of the welding process to its end for different travel velocities (30, 40, 60 mm/min) and different rotation velocities of the tool welding (1000, 1225, 1525 rpm). The results indicate a decrease in temperature with an increase in the travel velocity of the trolley carrying the models and a constant rotational velocity, and this indicates a noticeable increase in temperature as the time spent in the welding process increases. It is clear from the results presented in Figure 9-a constant rotational velocity (1000 rpm) that the highest temperatures were at the traveling velocity (30 mm/min) and the time taken for the welding process (3 minute). Also, the Figure 9-b in which the constant rotational velocity was (1225 rpm) and at different travel velocity (30, 40, 60 mm/min) shows an increase in temperatures with the passage of welding time and highly during the first thirty seconds from the start of the welding process, and after that the increase is in the form of a curve and it was higher an increase in temperature when the travel velocity was (30 mm/min), where the highest value (375 °C) was recorded after a time of (3) minutes after the welding process started. Figure 9-c where the rotational velocity was constant (1525 rpm) and at different travel velocity (30, 40, 60 mm/min) shows a marked increase in temperatures with the passage of welding time and at a high velocity during the first thirty seconds of the start of the welding process and then the increase is in the form of a curve. The highest temperatures in the welding processes were recorded when the travel velocity was (30 mm/min), where the highest value was (385) after the time (3) minutes from the start of the welding process.

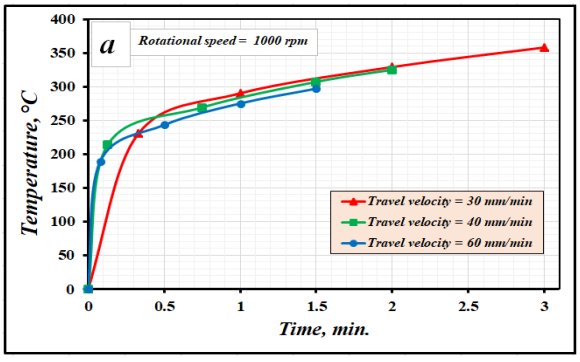

THE ANNALS OF "DUNAREA DE JOS" UNIVERSITY OF GALATI
FASCICLE IX. METALLURGY AND MATERIALS SCIENCE
N°. 1 - 2024, ISSN 2668-4748; e-ISSN 2668-4756
Article DOI: https://doi.org/10.35219/mms.2024.1.04

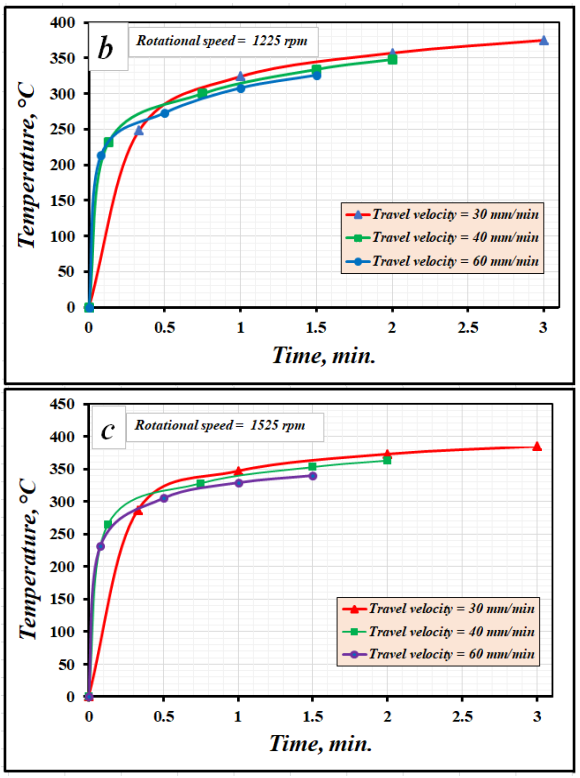

Fig. 9. *shows the relationship between temperatures with time from the starting of the friction stir welding process to its end when the rotational velocity is fixed and the travel velocity change*

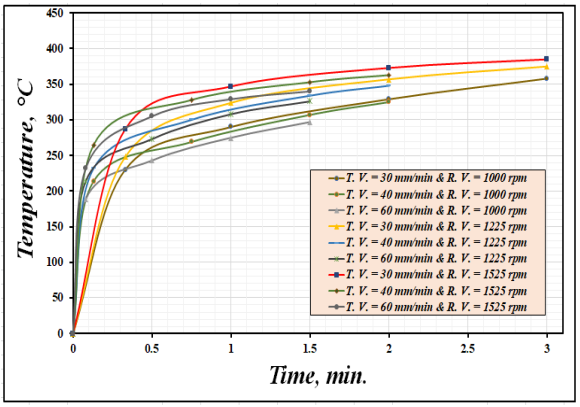

Fig. 10. *Shows the temperature change over time from the starting of the welding process to its end, at variable velocities of travel and rotational*

Figure 10 shows the relationship between the time spent in the friction stir welding process of the two alloys from the starting of the welding process to its end with the temperature distribution on the welded models on the vertical line of the welding process from the starting point of the welding process to its end for different rotation velocities of the welding tool (1000, 1225, 1525 rpm) and different travel velocities of the milling trolley (30, 40, 60 mm/min). The results indicate an increase in the temperature with an increase in the time spent in the friction stir welding process, where the highest degree and its amount (385 ºC) was recorded when comparing all the results obtained from the friction stir welding processes at different rotational velocities of the welding tool as well as different travel velocities.

3.3. Effect of constant of travel velocity and change of rotational velocity

The results obtained in Figure 7 were analysed in the Excel program to compare these results with the Figures 11 and 12. Figure 11 shows the results of the relationship between the time spent in the welding process, mixing friction, during the welding process from its starting to its end with the temperatures on the vertical line in the welding area, at different travel velocity of the carriage (30, 40, 60 mm/min), and different rotational velocity of the welding tool (1000, 1225, 1525 rpm). It is appeared from the results presented in Figure 11-a, at a constant travel velocity (30 mm/min) that the highest temperatures were at the travel velocity (1525 rpm) and the time taken for the welding process three minutes and it value (385 °C). Also, Figure 11-b, in which a constant travel velocity (40 mm/min) and a different rotational velocity (1000, 1225, 1525 rpm) was shown to increase in temperatures with the passage of welding time and at a high degree. During the first thirty seconds of starting the welding process and after that the increase will be in the form of a curve and the temperature increase will be higher when the travel velocity was (40 mm/min) and rotational velocity (1525 rpm), where the highest value (363 °C) after a time of two minutes after the start of the friction stir welding process.

Figure 11-c where the travel velocity was constant (60 mm/min) and at a different rotational velocity (1000, 1225, 1525 rpm) , the results indicate that the highest temperature was recorded when the rotational velocity was (1525 rpm) and the highest value was recorded (340 ºC) after a time of minute and a half, and this indicates that the increase in the rotational velocity and the increase in the travel velocity leads to an increase in temperatures during the welding process.

THE ANNALS OF "DUNAREA DE JOS" UNIVERSITY OF GALATI
FASCICLE IX. METALLURGY AND MATERIALS SCIENCE
Nº. 1 - 2024, ISSN 2668-4748; e-ISSN 2668-4756
Article DOI: https://doi.org/10.35219/mms.2024.1.04

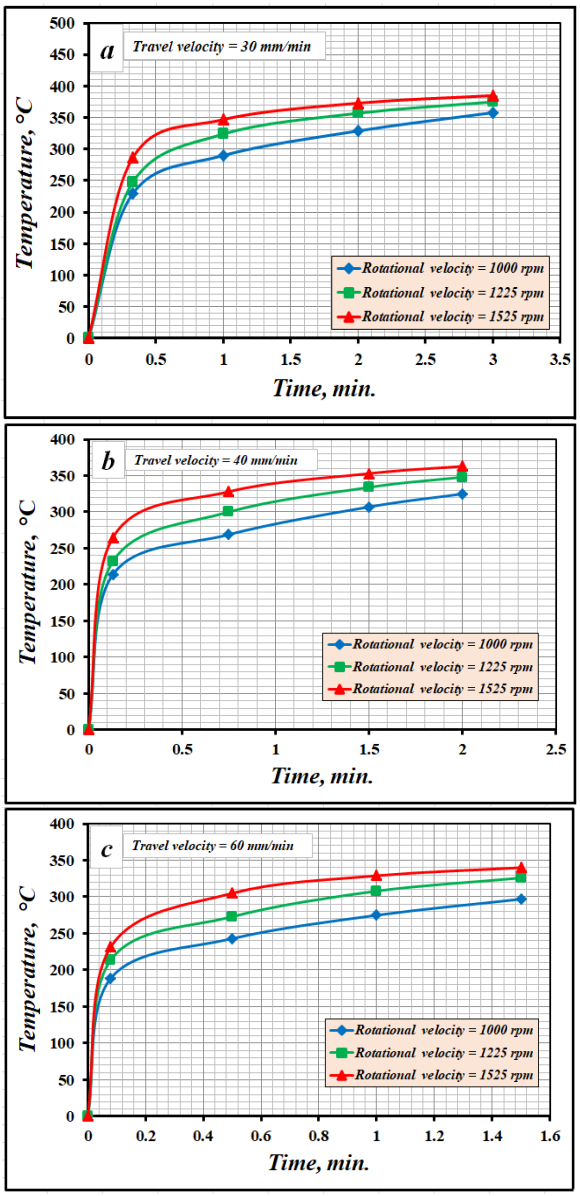

Fig. 11. *Shows the relationship between temperature and time taken in the welding process from starting to end, with constant travel velocity and change in rotational velocities of the welding tool*

Figure 12 shows the relationship between the time spent in the welding process of the two alloys using the friction stir welding method from its beginning to its end with the temperature distribution on the welded models on the vertical line of the welding process from the starting point of the welding process to its end for different travel velocity (30, 40, 60 mm/min) and each at a different rotation velocity of the welding tool (1000, 1225, 1525 rpm). The results indicate an increase in the temperature with an increase in the rotational velocity of the welding tool at constant travel velocity, and this indicates a significant increase in temperature with the increase in the rotational velocity.

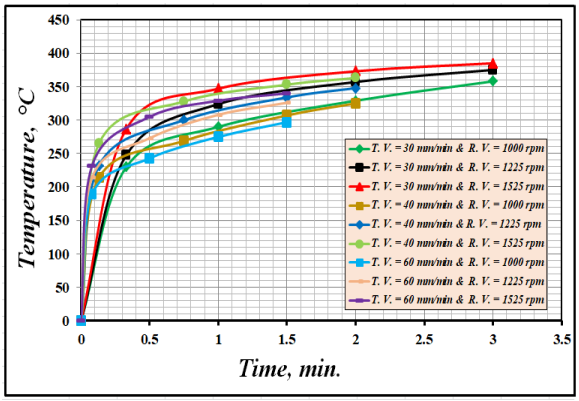

Fig. 12. *Shows the temperature change over time from the starting of the welding process to its end, at variable velocities of travel and rotational*

3.4. Effect of change travel velocity

Figure 7 shows the areas that have been identified in which the temperatures were measured during the friction stir welding process on a horizontal line in the middle of the models at constant rotational velocity of welding tool, and Figures 13 and 14 show those results.

Figure 15 shows the analysis of results when fixing the rotational velocity of the welding tool at (1000, 1225, 1525 rpm) and changing the travel velocity of the welding cart at each rotational velocity to compare between them, and the Figure 13-a shows the results of the temperature distribution when the rotational speed of the welding tool was (1000 rpm) and the travel speed of the welding cart (30, 40, 60 mm/min) It is evident from the figure that the highest temperature was recorded when the travel velocity of the welding cart was (30 mm/min), where the highest temperature was recorded in the welding centre and its value was (319 ºC), while the lowest temperature recorded in the welding centre was when the travel velocity was (60 mm/min) and its value was (270 ºC). Figure 14-b shows when the rotational velocity of the welding tool was constant at (1225 rpm) and the travel velocity of the welding cart was variable (30, 40, 60 mm/min), where the results showed that the highest temperatures were recorded when the travel velocity of the welding cart was (30 mm/min) and it was the highest value in the welding centre its value is (354 ºC), while the lowest value was recorded in the welding centre when the travel velocity of the welding cart was (60 mm/min) and its value was (308 ºC). Figure 14-c shows the temperature distribution

THE ANNALS OF "DUNAREA DE JOS" UNIVERSITY OF GALATI
FASCICLE IX. METALLURGY AND MATERIALS SCIENCE
Nº. 1 - 2024, ISSN 2668-4748; e-ISSN 2668-4756
Article DOI: https://doi.org/10.35219/mms.2024.1.04

when the rotational velocity of the welding pen was (1525 rpm) and the travel velocity of the welding cart is (30, 40, 60 mm/min), and it is clear from the figure that the highest temperature recorded in the welding centre was when the travel velocity of the welding cart was (30 mm/min) and its value was (375 ºC), while the lowest value was recorded in the welding centre when the travel velocity of the welding cart was (60 mm/min) and its value (335 ºC).

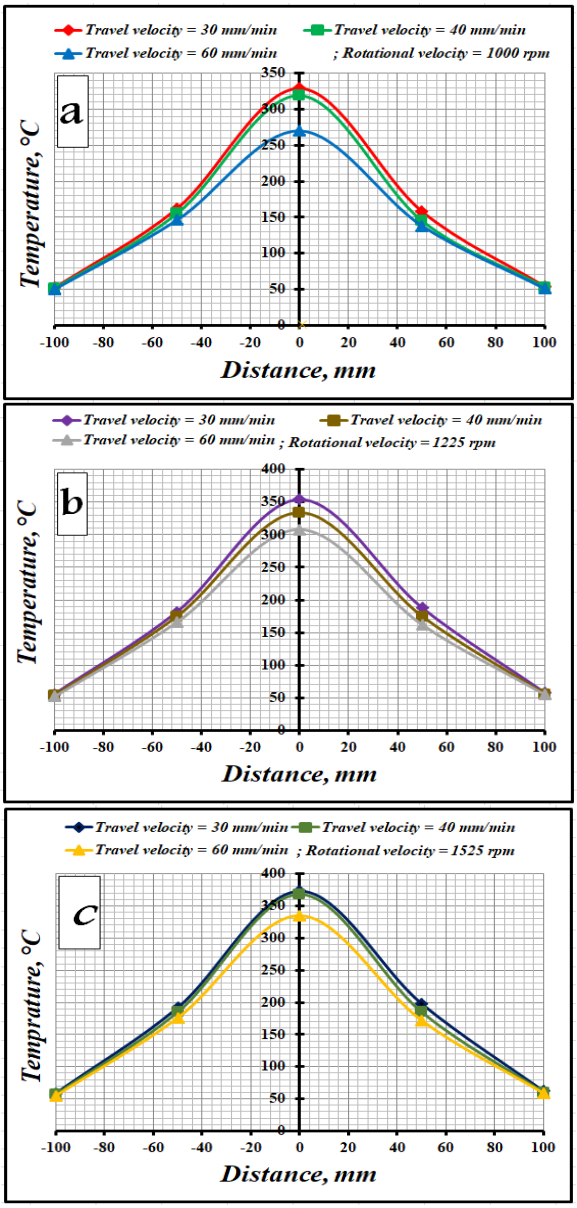

Fig. 14. *The temperature distribution with the distance from the welding centre of the two alloys on the horizontal line located in the middle of the two models: a. at T.S. = 1000 rpm, b. at T.S. = 1225 rpm, c. T.S. = 1525 rpm*

Figure 15 shows the results of the temperature distribution on the surface of the two alloys welded together in the friction stir welding method when the rotational velocity was variable (1000, 1225, 1525 rpm) and the travel velocity of the welding car was also variable (30, 60, 40 mm/min), and it appears from the figure that the highest temperatures it was recorded when the rotational velocity of the welding stylus was (1525 rpm) and the rotational velocity of the welding cart (60 mm/min) where the highest value was recorded in the welding centre and its value was (373 ºC) at these velocities. While the lowest value was recorded in the welding centre and its value was (270 ºC) when the rotational velocity of the welding tool was (1000 rpm) and the travel speed of the welding cart was (60 mm/min). This indicates that when the rotational velocity of the welding tool is constant and the travel velocity of the welding car changes, the temperatures decrease with the increase in the travel velocity of the welding cart, and the temperature increases with the increase in the rotational velocity of the welding tool.

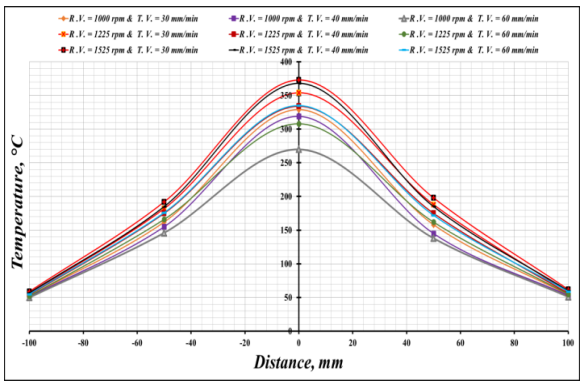

Fig. 15. *Shows the temperature distribution with distance along the weld horizontal line on the centre of the models: R.V. = 1000 ,1225 ,1525 rpm*

3.5. Effect of change rotational velocity of welding tool

Figure 7 shows the areas that have been identified in which the temperatures were measured during the friction stir welding process on a horizontal line in the middle of the models at constant travel velocity of milling cart, and Figures 16 and 17 show those results.

Figure 16 also proves these results. The (a, b, c) Figures that make up this figure show a noticeable increase in temperatures with an increase in the rotational velocity of the welding tool.

THE ANNALS OF "DUNAREA DE JOS" UNIVERSITY OF GALATI
FASCICLE IX. METALLURGY AND MATERIALS SCIENCE
No. 1 - 2024, ISSN 2668-4748; e-ISSN 2668-4756
Article DOI: https://doi.org/10.35219/mms.2024.1.04

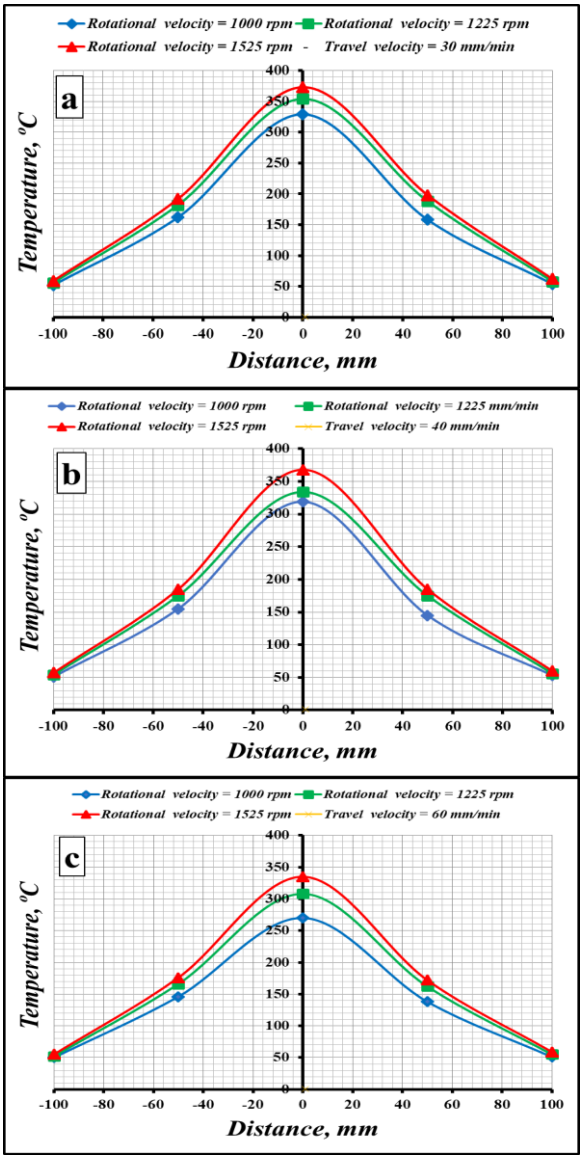

Fig. 16. *The temperature distribution with the distance from the welding centre of the two alloys on the horizontal line located in the middle of the two models: a. at T.V. = 30 mm/min, b. at T.V. = 40 mm/min, c. T.V. = 60 mm/min*

Figure 17 shows the results of the temperature distribution on the horizontal line passing through the middle of the models when the travel velocity of the welding cart is constant at (30, 60, 40 mm/min) and in each of them the rotary speeds of the welding stylus are changed by three different speeds which are (1000, 1225, 1525 rpm), and it appears from the figure that the highest temperatures were recorded when the travel velocity of the welding cart was equal to (60 mm/min) and the rotational speed of the welder was (1525 rpm) where the highest value was recorded in the centre of welding and its value was (373 ° C) at these speeds. While the lowest value was recorded in the welding centre and its value (270 °C) when the travel speed of the welding cart (60 mm/min) and the rotational speed of the welding tool (1000 rpm). This indicates that when the travel speed of the welding cart is constant and the rotating speed of the welding tool changes at it, the temperature increases with the increase in the rotational speed of the welding pen when the travel speed of the welding car remains constant, and the reason for this is the intensity of friction between the welding tool and the welded metal.

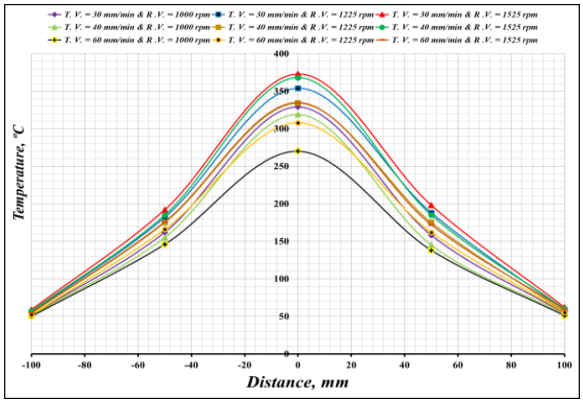

Fig. 17. *Shows the temperature distribution with distance along the weld horizontal line on the centre of the models: T.V. = 30, 40, 60 mm/min*

4. Conclusions

After conducting practical experiments for welding the models using the friction stir welding method, and after studying, analysing and discussing the practical results extracted from them, the following conclusions can be drawn:

1. The results showed that when the rotational speed is increased, the temperatures increase at constant travel velocity and the temperatures decrease when the travel velocity increases at constant rotational speed.

2. The lowest temperature recorded from the beginning to the end of welding was (287 °C) at a rotational speed (1000 rpm) and a constant travel speed (60 mm/min) and the time taken in the welding process was three minutes. The highest temperature recorded horizontally in the middle of the two alloys from the centre of the weld to the edges of the two alloys was in the welding area and its value was (373 °C) at a rotational speed (1225 rpm) and a constant travel speed (30 mm/min) while the lowest temperature was recorded horizontally in the middle of the two alloys From the weld centre to the edges of the alloy (270 °C) at a rotational velocity (1000 rpm)

and a constant travel velocity (60 mm/min), we notice that the temperatures decrease as we move away from the welding line.

3. The temperature distribution of both alloys is close to the similarity of the alloy properties, and that the temperatures of the alloy of the advance side are higher than the temperatures of the alloy of the retreating part.

4. We note the convergence of the theoretical results with the applied results.

Acknowledgment

This research was supported by Engineering Science Research Program through the Northern Technical University/ Technical Engineering college and Technical Institute of Mosul funded by the Ministry of Higher Education and Scientific Research / Republic of Iraq. (No. 00233- 2022).

References

[1]. Reynolds A. P., Tang W., Khandkar Z., Khan J. A., Lindner K., *Relationships between weld parameters, hardness distribution and temperature history in alloy 7050 friction stir welds*, Science and Technology of Welding and Joining Journal, 10 (2), p. 190-199, 2005.

[2]. Takashi Nakamura, Toshiyuki Obikawa, Eitaro Yukutake, Satoru Ueda, Itaru Nishizaki, *Tool Temperature and Process Modeling of Friction Stir Welding*, Modern Mechanical Engineering, 8, p. 78-94, 2018.

[3]. Masoud Jabbari, *Effect of the Preheating Temperature on Process Time in Friction Stir Welding of Al 6061-T6*, Journal of Engineering, p. 1-5, 2013.

[4]. Silva A. C. F., De Backer J., Bolmsjö G., *Temperature measurements during friction stir welding*, Int J Adv Manuf Technol, 88, p. 2899-2908, 2017.

[5]. Oussama Mimouni, Riad Badji, Mohamed Hadji, Afia Kouadri-David, Hamel Rachid, Nabil Chekroun, *Numerical Simulation of Temperature Distribution and Material Flow During Friction Stir Welding 2017A Aluminum Alloys*, MATEC Web of Conferences, 80, p. 1-8, 2016.

[6]. Iordache Monica, Nitu Eduard, Badulescu Claudiu, Iacomi Doina, Botila Lia, Radu Bogdan, *Evaluation of Thermal Distribution in Friction Stir Welding on Dissimilar Materials (Cu-Al) Using Infrared Thermography and Numerical Simulation*. Trans Tech Publications, 1138, p. 113-118, 2016.

[7]. Padmanaban R., Ratna Kishore V., Balusamyc V., *Numerical Simulation of Temperature Distribution and Material Flow During Friction Stir Welding of Dissimilar Aluminum Alloys*, Procedia Engineering, 97, p. 854-863, 2014.

[9]. Dan Birsan, Danut Iordachescu, Jose Luis Ocana, Pedro Vilaca, *Fem model for friction stir welding of aluminum*, The Annals of "Dunarea de Jos" University of Galati Fascicle XII, Welding Equipment and Technology, Year XIX, ISSN 1221-4639, 2008.

[10]. Peel M. J., Steuw Er A., Withers P. J., Dickerson T., Shi Q., Shercliff H., *Dissimilar Friction Stir Welds in Aa5083-Aa6082*, Metallurgical and Materials Transactions A, 37, p. 2183-2193, 2016.

[11]. Yuh J. Chao, Qi X., Tang W., *Heat Transfer in Friction Stir Welding-Experimental and Numerical Studies*, Journal of Manufacturing Science and Engineering, 125, p. 138-145, 2003.

[12]. Shabbir Memon, Jacek Tomk ów, Hesamoddin Aghajani Derazkola, Thermo-Mechanical Simulation of Underwater Friction Stir Welding of Low Carbon Steel. Materials, 14, p. 1-17, 2021.

[13]. Bindu M. D., Tide P. S., Bhasi A. B., *Numerical Studies on Temperature and Material Flow During Friction Stir Welding using Different Tool Pin Profiles*, Journal of Advanced Research in Fluid Mechanics and Thermal Sciences, 83, p. 91-104, 2021.

[14]. Vishwanath M. M., Lakshamanaswamy N., Ramesh G. K., *Numerical Simulation of Heat Transfer Behavior of Dissimilar Aa5052-Aa6061 Plates in Fiction Stir Welding: An Experimental Validation*, Journal of Mechanical Engineering, 2019, 69: pp. 159 – 170.

[15]. En-zhi Gao, Xing-xing Zhang, Chun-zhong Liu, Zong-yi Ma, *Numerical simulations on material flow behaviors in whole process of friction stir welding*, Trans. Nonferrous Met. Soc. China, 28, p. 2324-2334, 2018.

[16]. Anton Naumov, Evgenii Rylkov, Pavel Polyakov, Fedor Isupov, Andrey Rudskoy, Jong-Ning Aoh, Anatoly Popovich, Oleg Panchenko, *Effect of Different Tool Probe Profiles on Material Flow of Al–Mg–Cu Alloy Joined by Friction Stir Welding*, Materials, 14, p. 1-14, 2021.

[17]. Amir Ghiasvand, Mahdi Kazemi, Maziar Mahdipour Jalilian, Hossein Ahmadi Rashid, *Effects of tool offset, pin offset, and alloys position on maximum temperature in dissimilar FSW of AA6061 and AA5086*, International Journal of Mechanical and Materials Engineering, 15, 6, p. 1-14, 2020.

[18]. Vermaa S., Meenua, Misra J. P., *Study on temperature distribution during Friction Stir Welding of 6082 aluminum alloy*, Materials Today, 4, p. 1350-1356, 2017.

[19]. Karash E. T. B., Yassen S. R., Kassim M. T. E., *Effect of friction stir welding parameters on the impact energy toughness of the 6061-t6 aluminum alloys*, Annals of "Dunarea de Jos" University, Fascicle XII ISSN 1221-4639 Welding Equipment and Technology, vol. 29, p. 27-32, 2018.

[20]. Abdul Arif, Chetan Swaroop, Pandey K. N., *Temperature Validation for Friction Stir Welding (Fsw) of Dissimilar Aluminum Alloys*, Proceedings of International Conference on Advances in Mechanical Engineering, p. 1-10, 2013.

[21]. Birsan D., Scutelnicu E., *Modelling of thermo-mechanical effects generated by friction spot stir welding process*, Annals of "Dunarea de Jos" University, Fascicle XII ISSN 1221-4639, Welding Equipment and Technology, vol. 25, p. 29-34, 2014.

[22]. Bušić M., Kožuh Z., Klobčar D., *Influence of the tool travel speed on friction stir processing of aluminum alloy AlCu4Mg1*, Annals of "Dunarea de Jos" University, Fascicle XII, ISSN 1221-4639, Welding Equipment and Technology, vol. 28, p. 11-14, 2017.

[23]. Cole E. G., Fehrenbacher A., Duffie N. A., Zinn M. R., Pfefferkorn F. E., Ferrier N. J., *Weld temperature effects during friction stir welding of dissimilar aluminum alloys 6061-t6 and 7075-t6*, Int J Adv Manuf Technol, 71, p. 643-652, 2014.

[23]. Birsan D., Scutelnicu E., Stan F., *Hardness of friction stir welded joints of AA-6061-t6 aluminum alloy*, Annals of "Dunarea de Jos" University of Galati, Fascicle XII, Welding equipment and technology, ISSN 1221-4639, vol. 21, 2010.

[24]. Nageeb Salman Abtan, Ataalah Hussain Jassim, Mustafa Shakir Marmoos, *Study on the Effects of Rotational and Transverse Speed on Temperature Distribution through Friction Stir Welding of AA2024- O Aluminium Alloy*, CFD Letters, 1, p. 55-69, 2019.

[25]. Kareem N. Salloomi, Furat I. Hussein, Sanaa N. M. Al-Sumaidae, *Temperature and Stress Evaluation during Three Different Phases of Friction Stir Welding of AA 7075-T651 Alloy*, Hindawi, p. 1-11, 2020.

[26]. Karash E. T., Ali H. M., Hamid A. F., *Mathematical Model for the Temperature Distribution on The Surface of Two Aluminum Alloys Welded by Friction Stir Welding*, Annals of "Dunarea de Jos" University of Galati Fascicle XII, Welding equipment and technology, ISSN 1221-4639, vol. 23, 2022.

[27]. Emad Toma Karash, Jamal Nayief Sultan, Majid Khaleel Najem, Amenah Faris Hamid, *Comparison of the Influence of Temperature Change Distribution of Three Surface Regions on the*

Hardness of Two Dissimilar Aluminum Alloys Welded by Friction Stir Welding, International Journal of Heat and Technology, vol. 40, no. 4, p. 1013-1023, August, 2022.

[28]. Emad T. B. K., Saeed R. Y., Mohammed T. E. Q., *The Effect of the Cutting Depth of the Tool Friction Stir Process on the Mechanical Properties and Microstructures of Aluminum Alloy 6061-T6*, American Journal of Mechanics and Applications, 3(5), p. 33-41, 2015.

[29]. Matweb, *Your Source for Materials Information*, https://www.matweb.com, 2000.

[30]. Mishra R., Murray S., Mahoney W., *Friction Stir Welding and Processing*, ASM International, USA, 2007.

[31]. ***, ASTM E 3 – 01, *Standard Guide for Preparation of Metallographic Specimens*, USA, 2001.

[32]. ***, ASM *Aerospace Specifications Metals Inc*. - retrieved 18 September 2019.

[33]. ***, Alcoa 2024 data sheet Archived 2006-08-27 at the Way back Machine (pdf), accessed October 13, 2006.